Soil Infiltration Rate Prediction using Machine Learning Regression Model: A Case Study on Sepinggan River Basin, Balikpapan, Indonesia

Totok Sulistyo and Rohmat Fauzi

Balikpapan State Polytechnics
Jln. Soekarno Hatta KM. 8, Batu Ampar, Balikpapan, Kalimantan Timur 76129

Corresponding author: totok.sulistyo@poltekba.ac.id
Manuscript received: November, 29, 2022; revised: February, 13, 2023;
approved: May, 31, 2023; available online: October, 10, 2023

Abstract - The infiltration rate of soil data is important in a wide range of planning, such as city planning, drainage design, landuse planning, flood prediction, flood disaster mitigation, *etc*. Collecting data of infiltration through in-site direct measurements is time consuming and costly. Indeed, inferring the infiltration rate using available parameters and the fittest model is needed. The model can shortcut the field measurement to get a predicted accurate infiltration rate that is worthy to support vital planning. This research aims to develop a model of infiltration rate based on initial water contents and grain size of soils. The results are three outstanding models based on the Multiple R Squared, Root Mean Square Error (RMSE), and Mean Average Error (MAE). The implication of the fittest model is reducing the cost and time to get the predicted infiltration rate. The field measurements can be skipped by sampling undisturbed soils and laboratory tests.

Keywords: infiltration rate, initial water contents, grain size

Introduction

Background

The infiltration rate of the soil is important in a hydrological cycle as it is controlling soil degradation by erosion in hilly and slope areas, runoff, and irrigation efficiency (Angulo-Jaramillo *et al.*, 2016), because the higher infiltration rate reduces soil erosion and runoff (Thomas *et al.*, 2022). Considering how important infiltration rate is in soil cultivation, soil conservation, and hazard mitigation, the infiltration rate has been modeled based on a artificial intelligence, such as artificial neural networks (ANN) (Sy, 2006), random forests (Sihag *et al.*, 2019; Bergeson *et al.*, 2022), support

vector machine (Sihag *et al.*, 2019), and machine learning (Khosravi *et al.*, 2022) to get a better correlation of a model to the infiltration with smaller root square mean of error. The soil infiltration will be influenced by slope and soil properties, such as soil moisture, grain size distribution, bulk density (Setiawan *et al.*, 2019), the availability of interconnected pores, and the saturation degree of soil. Not only pore spaces between grains, but cracks in the soil also play an important role as conduits in the infiltration of water into the soil (Ma *et al.*, 2022). Such cracks and macropores in the soil and geological formation are provided by biological activities (Fueki *et al.*, 2012), anthropogenic, weather, and geological structure, such as

joints and faults. Studies on the correlation between infiltration rate and the partial properties of soil have been carried out by previous researchers. The high initial water moisture in the soil causes a low infiltration rate, and there is a correlation between wet soil and low infiltration rate (Bhave and Sreeja, 2013; Ruggenthaler *et al.*, 2016; Kiptiah *et al.*, 2020). Meanwhile, the presence of clean sand has a greater pore space and increases infiltration capacity (Michael, 2010), and the presence of silt and clay or matrix between grains will reduce the volume of pore space of soil, so the infiltration rate will decrease. Otherwise, the presence of swelling clay will increase sorptivity and infiltration rate of red-brown soil (McIntyre and Sleeman, 1982). The decreasing infiltration capacity of soil causes increasing runoff water, and becomes a flood potency in the area. The infiltration also increases soil saturation and positive pore water pressure, meanwhile it decreases pore water suction and they will reduce the safety factor of slope and induce slope failure (Muntohar *et al*., 2022; Sugianti *et al*., 2022). The infiltration rate of the Balikpapan area based on a previous research is 12 mm/hour up to 240 mm/hour (Juwita and Santoso, 2019). A study about parameters that determine the infiltration rate is needed for better natural water recharge management, flood analysis, irrigation planning, urban planning, *etc*. (Dahan *et al.*, 2007).

Infiltration is also part of the natural recharge process in a catchment area. Water flows into the ground and flows deep down into the aquifer, so the sustainability of the aquifer also depends on the rate of infiltration in the recharge area (Alencoão and Pacheco, 2006). The impact of infiltration rate on the sustainable and livable city can not be neglected, as infiltration in the rainfall-runoff model determines the flood potency of the area. Thus, the study of stormwater and its connectivity to the low infiltration rate is needed (Bergeson *et al.*, 2022). It is also the initial process of storing rainwater as groundwater (Alencoão and Pacheco, 2006). The drainage design should take the infiltration as well as runoff into account to avoid floods or water overflows during the rainy season. The problem of carrying out field measurements of infiltration in a wide area of interest is costly and time-consuming. Therefore, an accurate model of infiltration rate using texture parameters is needed (Khosravi *et al.*, 2022). This research aims to model the correlation between infiltration capacity to the initial water content, silt content, and clay content. The results of this research can be applied in infiltration rate prediction to replace costly and time-consuming *in situ* measurement. The reliable model is also expected to improve the ANN model (Sy, 2006) which is hiding its formula.

Geological Settings

Geologically, the researched area is situated in Kutai Basin. Stratigraphically, it has Pleistocene Kampung Baru Formation consists of sandy claystone, intercalation of coal and marl, and limestone. Underneath, Late Miocene Balikpapan Formation comprises alternation of quartz sandstone, silty claystone, and intercalation of shale and marl. Pulau Balang Formation is dominated by quartz and greywacke sandstone (Hidayat and Umar, 1994; Sulistyo, 2018; Formansya *et al.*, 2020). Kampung Baru and Balikpapan Formations outcrop in the southern Balikpapan. Meanwhile, Balikpapan Formation and part of Pulau Balang Formation are exposed in the northwest area. The uppermost geological unit is Quarternary alluvium deposits, which contain mixed deposits of silt, sand, and gravel (BAPPEDA Balikpapan, 2002; Sulistyo and Abrar, 2017) as depicted in Figure 1. Soil and recent deposits are a result of decomposition, disintegration, and deposition process of its underlying geologic formation. Geohydrologically, the area is the recharge and discharge areas of Balikpapan City.

Regionally, almost all the rock formation of the area had been deformed, with age span from Pretertiary to Late Tertiary. The results of tectonism are joints, faults, anticlines, and synclines. Tertiary rock formation is folded with dip angles between 10° to 40°, while the dip angle of Pretertiary rocks is more than 40°. The trend of axial folds are north-south to northeast-southwest. They are characterized by normal fault, thrust, and strike-slip faults. Tectonic events of the area are predicted to occur since the Jurassic time (Hidayat and Umar, 1994).

Hydrogeology of the researched area is characterized by confined aquifer, perched aquifer,
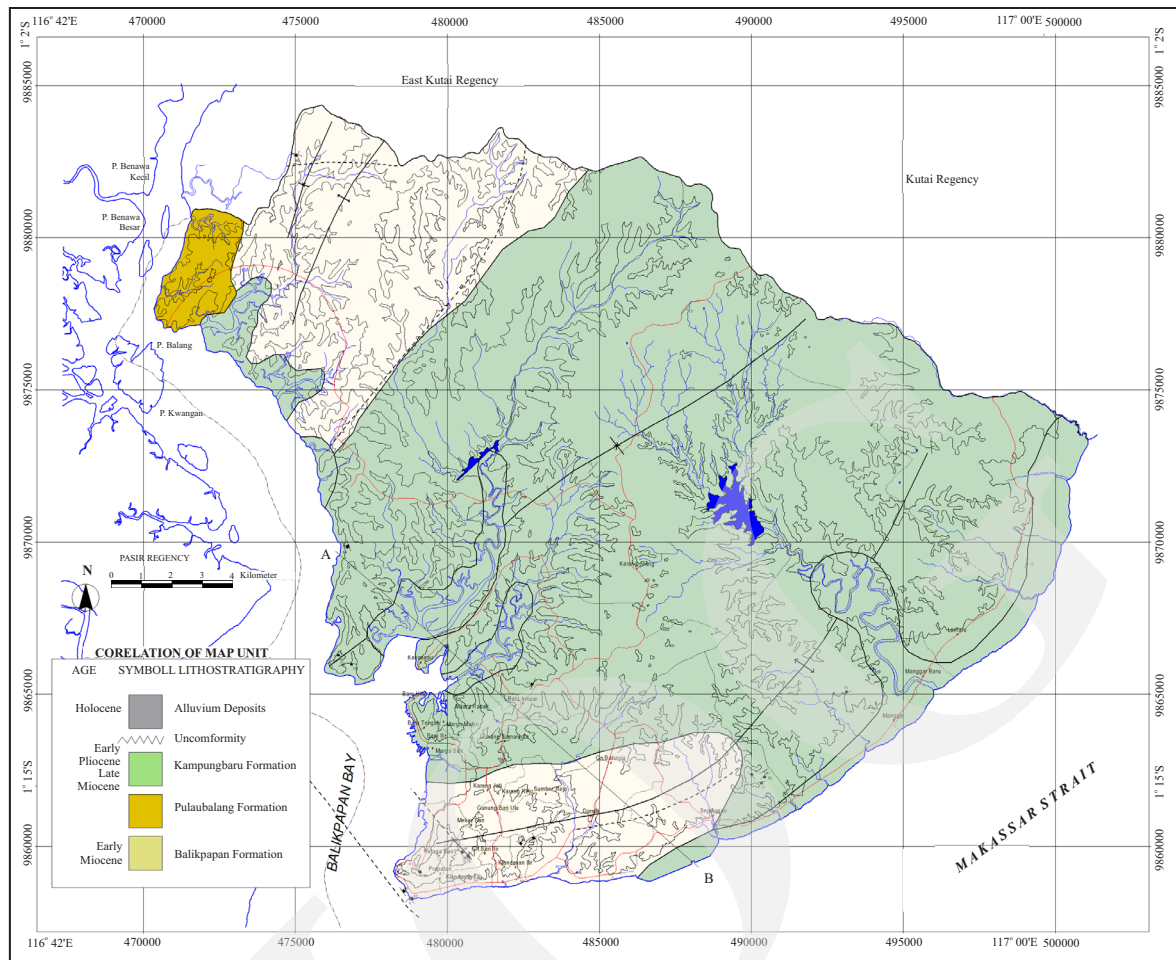
Figure 1. Geological map of Balikpapan City (BAPPEDA Balikpapan, 2002).

and free aquifer. Many springs are also found in southern Balikpapan area. Such springs are interpreted as the result of perched aquifers that have been intersected by topography. The existence of perched is caused by impermeable lens of claystone in thick sandstones of Balikpapan Formation. Therefore, it can stop water infiltrates deep down and store water as shallower groundwater (Sulistyo, 2003). Such condition is portrayed in Figure 2.

METHODS AND MATERIALS

Methods

The research activities consisted of field measurement and sampling, laboratory tests, and studio works. The methodology of this research is depicted in Figure 3.

Literature review and gap analysis are the stages of reviewing previous studies and finding the gaps to find the novelty. Then, gaps are converted to the problem statement, and field reconnaissance. Sampling location planning is conducted to get representative location and samples of the area. The next stage is the preparation of tools and materials for *in-situ* tests and sampling which consists of composite soil sampling and infiltration measurements. The next step is laboratory analysis for the initial water content of the soil sample, sieve, and hydrometer test, then the analysis of grain gradation and soil classification. The result of field measurements was analyzed using the Horton Method. The result of the test that consists of infiltration capacity (IR), initial water content (IWC), and percentage of sand, silt, and clay was analyzed using machine learning model regression in R
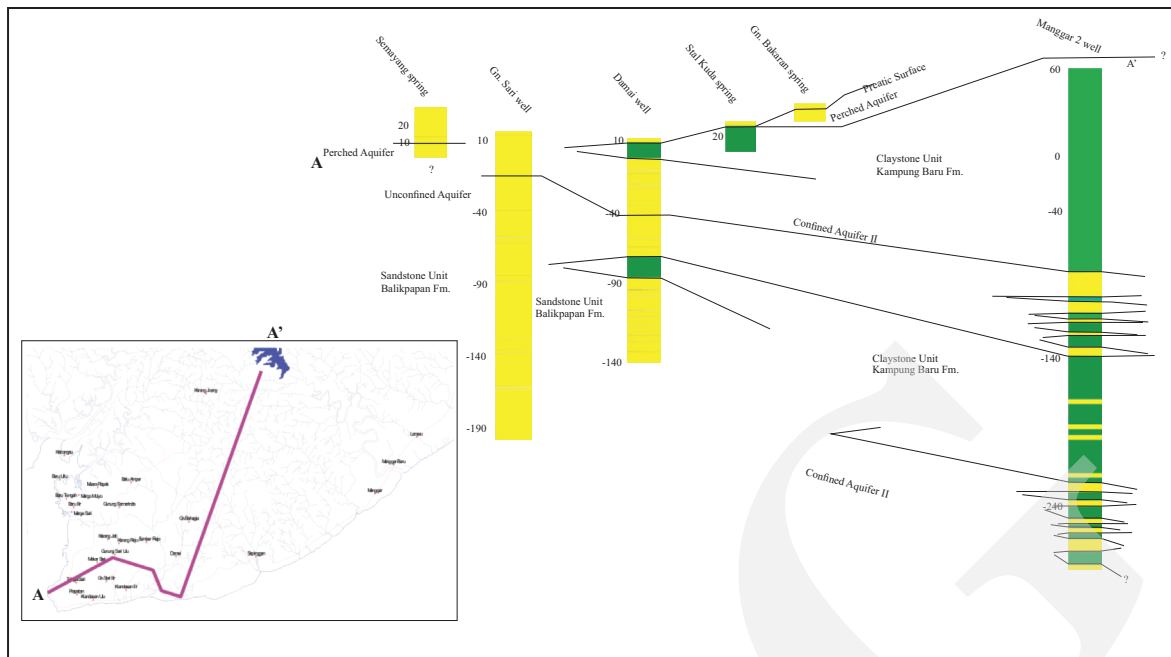
337

Figure 2. Correlation of deep well log and outcrops in Balikpapan (Sulistyo, 2003).
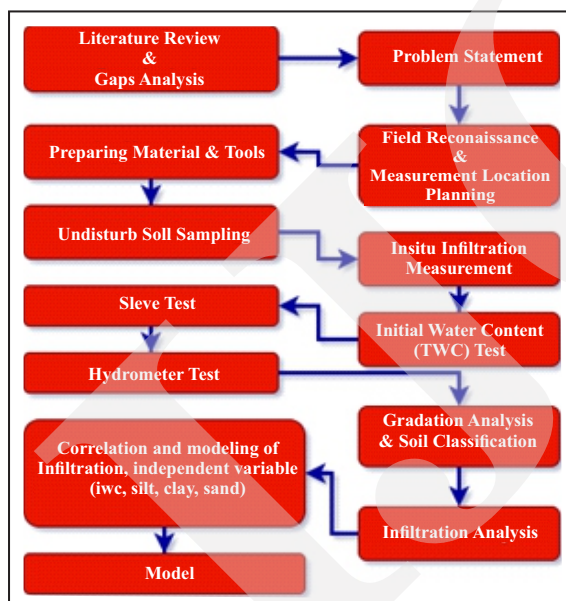

Figure 3. Research methodology.

Studio to get a fit model. In this analysis, simple regression and models are employed based on Formula 1 as below.

$$y = \beta_o + \beta_1 x_1 + \cdots + \beta_n x_n + \epsilon \quad ....(1)$$

where:

y = predicting infilltration rate dependent variable

β_o = intercept value

β_1 and β_n = coeficient of independent variable x_1 and x_n

ϵ = estimated error

The infiltration rate (IR) is the dependent variable that will be predicted, while independent variables are the combination of variables and a single variable as portrayed in Table 1.

Performance parameters that are used in assessing model accuracies consisted of RMSE,

Table 1. Combination of Variables and Single Variables in Regression Model

Model	Dependent Variable(s)
1	IWC, Silt, Clay, Sand
2	IWC, Silt, Clay
3	IWC, Silt, Sand
4	IWC, Clay, Sand
5	IWC, Sand
6	IWC, Silt
7	IWC, Clay
8	IWC
9	Silt
10	Clay
11	Sand

MAE, and Coefficient of Determination (R2). Therefore, the most reliable model can be determined. To get such values, Formula 2, 3, and 4 are used. The RMSE is defined as follows:

$$RMSE = \sqrt{\frac{1}{n}\sum_{i=1}^{n}(Y_{pi} - Y_{oi})^2} \quad ....(2)$$

MAE is calculated as follows:

$$MAE = \frac{1}{n}\sum_{i=1}^{n}|Y_{pi} - Y_{oi}| \quad ....(3)$$

AN R^2 is calculated as follows:

$$R^2 = \frac{\sum_{i=1}^{n}(Y_{oi}-\bar{Y})(Y_{pi}-\tilde{Y})}{\sqrt{\sum_{i=1}^{n}(Y_{oi}-\bar{Y})^2 \sum_{i=1}^{n}(Y_{pi}-\tilde{Y})^2}} \quad ....(4)$$

where:

Y_o is the observed infiltration rate,

Y_p is the predicted infiltration rate,

$\bar{Y}$ is the average observed infiltration rate, and

$\tilde{Y}$ is the average predicted infiltration rate.

RMSE depicts the differences between the observed value and predicted value, and it gives more weight to the larger error and vice versa. Meanwhile, MAE shows the average (Khosravi *et al.*, 2022). R^2 is a statistical measure that depicts the goodness of the model to the actual infiltration rate (Sy, 2006).

Materials

Tool and material for *in-situ* measurements that were used during the research consisted of a double ring infiltrometer, stopwatch, ruler, nozzle, water barrel, camera, GPS, and water as material, and sampling needs auger, PVC pipe as sample wrap, and marker. The laboratory analysis needs sieves, sieve shaker, digital scale, plate, oven, mixer, hydrometer, sedimentation cylinders, jars, thermometer, beaker, and sodium silicate. For the data analysis, R Studio 1.4 was used.

The observation, measurements, and sampling were carried out in Sepinggan River Basin. Administratively, the area is located in southern Balikpapan District, Balikpapan City, East Kalimantan Province, Indonesia. The locations of the field measurement and sampling are depicted on the map as shown in Figure 4.

The result observation from fourteen stations showed that the average infiltration rate of 1.57 up to 5.66 cm/hour was classified as medium to rather slow. The average infiltration capacity at each location of observation is depicted in Figure 5. Three rather slow infiltration observations were located relatively downstream, meanwhile medium infiltration observations were located upstream (Figure 6).

The depth (Δh) in infiltrometer of fourteen observations started from 5 to 13 cm in 7.5 minutes, and it was constant after 45 minutes up to 1 hour (Figure 7).

Undisturbed samples taken using hand auger from 0.5 up to 1 m depth, were tested in the laboratory to get initial water contents using ASTM D2216 Procedure. Soil samples have the initial moisture of 17 up to 48.77%. Initial Water Content (IWC) for each sample is shown in Table 2.

Undisturbed samples were also tested for their grain size distributions of each sample using a sieve and hydrometer test. The result of field measurements and laboratory tests is consisted of infiltration capacity, IWC, and percentage of sand, silt, and clay. The percentage of sand, silt, and clay of each soil sample can be classified using the Ternary USDA classification diagram based on its textural properties using the R script as depicted in Figure 5. Most samples were classified as sandy clay loam, and the rest were classified as clay loam, sandy loam, loamy sand, and sand.

The data was prepared and cleaned for further analysis. The outlier was identified using the box plot function in R Studio, and all number of variables found one outlier in the infiltration variable. The identification of the outlier is illustrated in
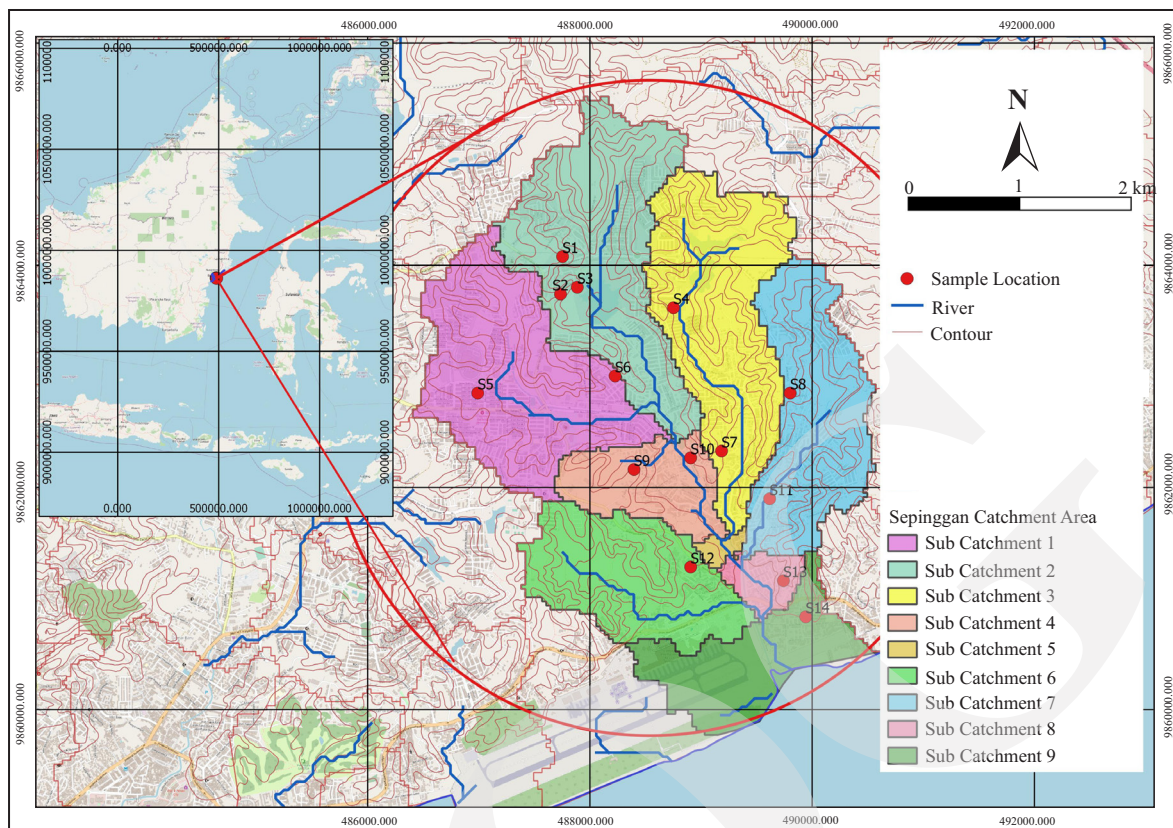
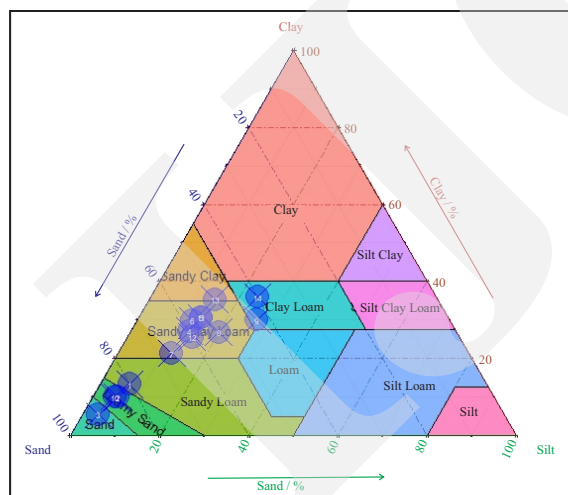Figure 4. Location of sampling and field observations.

Figure 5. Soil texture of samples based on USDA textural classification chart.

Figure 8. Then, outlier and its pairs in the row were excluded from the modeling in multiple regression analysis. The result of cleaning data from fourteen samples, there was one outlier of infiltration rate in the location of S1, so the useable data was the observation from location S2 up to S14. In the next step after cleaning data, it was then divided randomly into 80% dataset as training data and 20% dataset as test data.

The correlation of infiltration rate and physical parameters of soil was modeled using simple regression and multiple regression, using machine learning in R Studio. The formula generated by Machine Learning was Regression Function of lm (formula $= y \sim x_i + x_{i+1} + \ldots + x_n$, data = training_set), and its summary is written in Table 3 using the following symbol.

From the output of regression, the strength of correlation between the dependent and independent variables of each model is listed in Table 4. The further analysis comparison of observed infiltration rates and the predicted infiltration rates is known as RMSE and MAE as portrayed in Table 4.

A previous research has detected in cultivated soil, where a single soil property of sand has the highest correlation to the infiltration rate compared to the other properties of soil, such as clay,
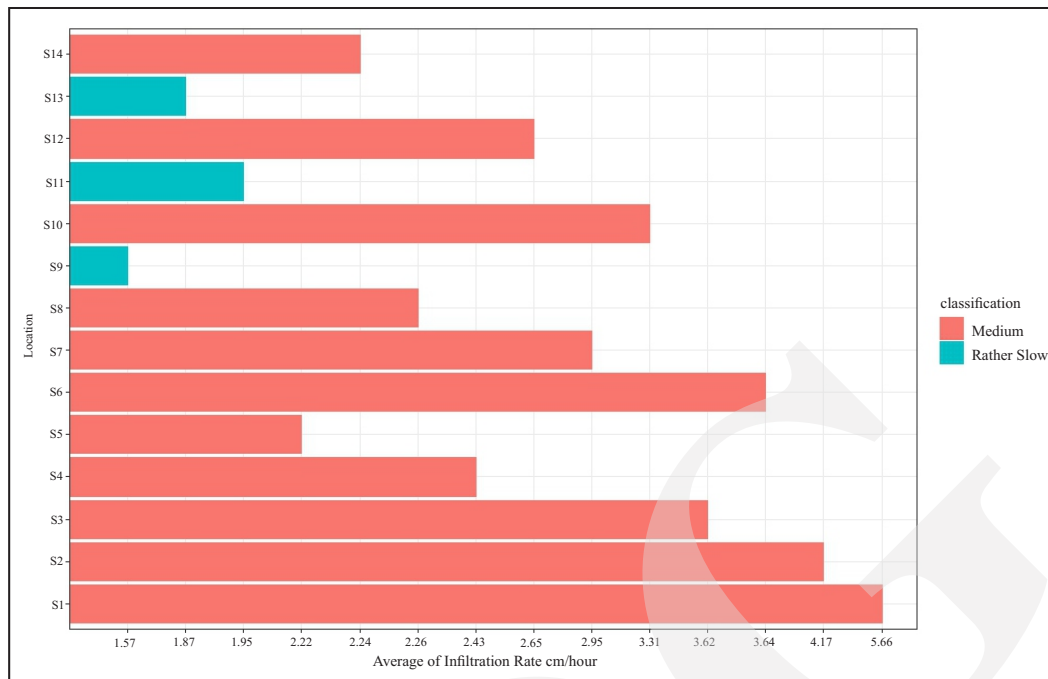
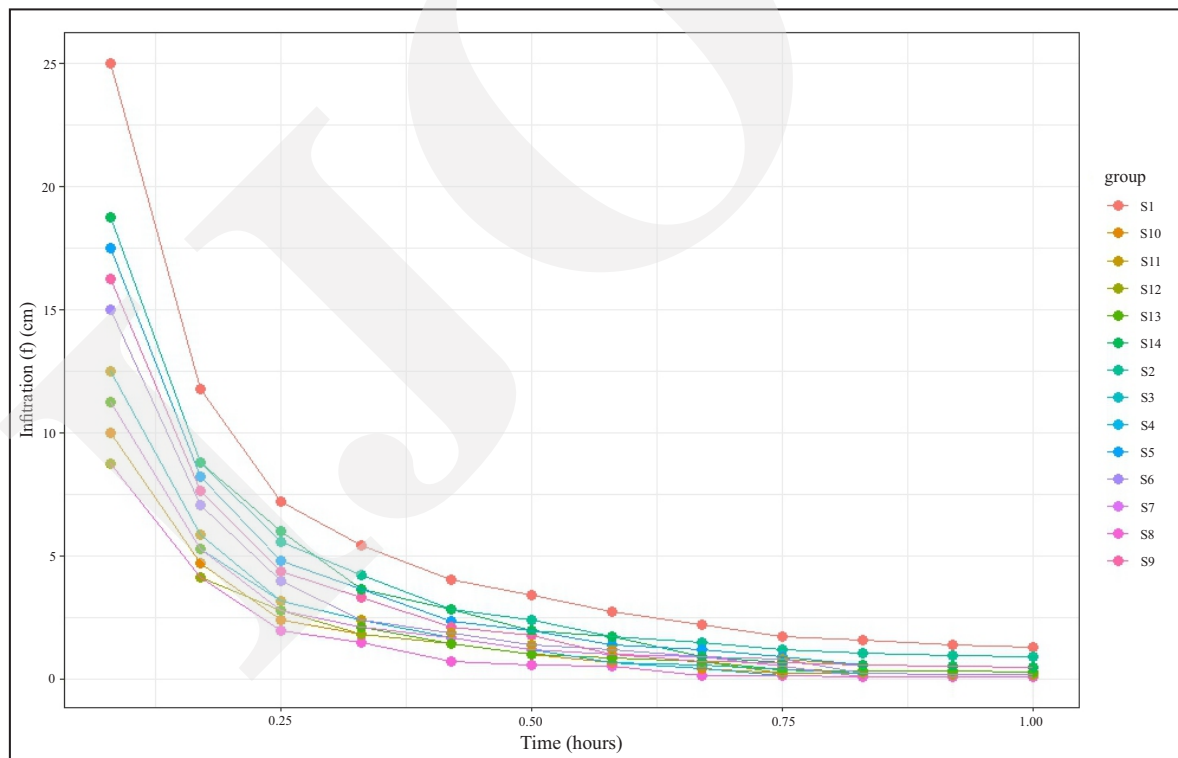Figure 6. Average infiltration capacity for each observation.

Figure 7. Infiltration rate (f) (cm) in 1 hour of observation in each location.

Table 2. IWC of Soil Samples

LOC	S1	S2	S3	S4	S5	S6	S7	S8	S9	S10	S11	S12	S13	S14
IWC (%)	17.0	22.54	21 .0	23.42	24.72	17.81	22.45	14.16	45.67	21.32	48.77	36.67	38.75	28.93
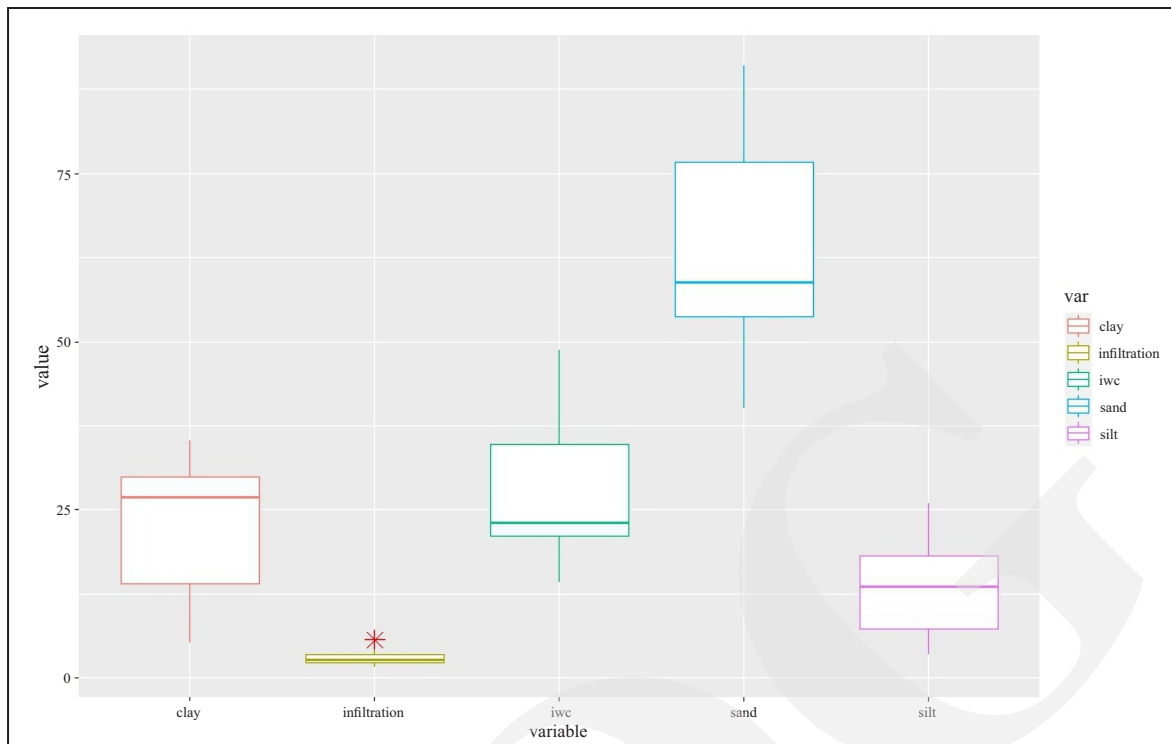
Figure 8. Box plot of the variable to identify outlier.

Table 3. Output of the Regression Function

Model	Formula
1	$y = 3.6954975 - 0.0008932\,x_1 + 0.0188830\,x_2 - 0.0672503x_3 + 0.0048447\,x_4$
2	$y = 4.1687807 - 0.0009843x_1 + 0.0144152x_2 - 0.0717995\,x_3$
3	$y = -0.58626 - 0.01009\,x_1 + 0.02695x_2 + 0.05009x_4$
4	$y = 4.638701 - 0.003752x_1 - 0.068914x_3 - 0.004316x_4$
5	$y = 0.621606 - 0.014539x_1 + 0.038490x_4$
6	$y = 4.56992 - 0.03010x_1 - 0.083162x_2$
7	$y = 4.235492 - 0.004696x_1 - 0.062215_{x3}$
8	$y = 3.78206 - 0.04059\,x_1$
9	$y = 3.86618 - 0.09074\,x_2$
10	$y = 4.156846 - 0.064260\,x_3$
11	$y = 0.01999 + 0.04184\,x_4$
	Explanation : y= infiltration, x_1= IWC, x_2= silt, x_3= clay, x_4= sand

silt, bulk density, and moisture content (Tikaram *et al.*, 2018). The coefficient of correlations, standard deviations, root mean square error, and model were compared, and analyzed using the Taylor diagram (Carslaw, 2019) as depicted in Figure 9.

DISCUSSION

The sampling could not be done using the grid method, because some locations were densely populated in an urban area, and others were not naturally deposited soil. Thus, the sampling and

Table 4. Multiple of R-Squared, RMSE, and MAE in Each Model

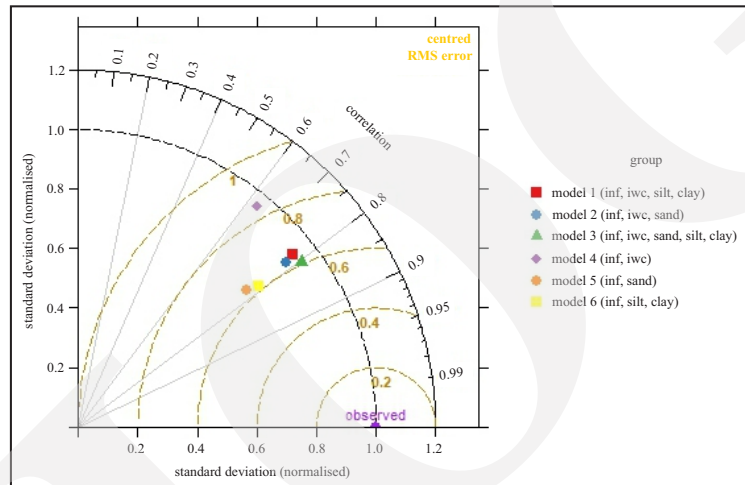| Model	Multiple R-Squared	RMSE	MAE
1	0.9222	0.4927443	0.31914
2	0.922	0.4933758	0.3189769
3	0.8955	0.400012	0.2806742
4	0.9206	0.4598607	0.2968624
5	0.8923	0.3683726	0.2607738
6	0.8393	0.360245	0.3022879
7	0.9204	0.4469914	0.2900606
8	0.2764	0.5884582	0.5017798
9	0.6922	0.4342064	0.3458374
10	0.9176	0.4683544	0.3005737
11	0.8624	0.4186181	0.2920075

Figure 9. Taylor diagram of model regression.

observation were carried out at random locations as depicted in Figures 3 and 4. The sampling locations are in the catchment area of Sepinggan River Basin, from the classification of infiltration rate of several measurement locations. It seems that the infiltration rate classification correlates the soil upstream and downstream of the river basin as depicted in Figure 4. The upstream has a greater infiltration rate rather than in downstream. To prove that, the correlation phenomenon needs further studies. The physical properties which consist of initial water content (IWC) and the grain size that have been observed in this research, are analyzed in their correlation to the infiltration rate by the regression models. Those models are listed in Table 3. The models of correlation have resulted from Machine Learning Regression Model using

R Studio. There are developed eleven models of correlation between Infiltration Rate as Dependent Variable, and IWC and Grain Size as Independent Variables (x_1 = IWC, x_2 = silt, x_3 = clay, and x_4 =sand). The fittest model is Model 1,

$$y = 3.6954975 - 0.0008932\,x_1 + 0.0188830\,x_2 - 0.0672503 x_3 + 0.0048447\,x_4 \quad \ldots\ldots\ldots\ldots(5)$$

which has the Multiple R Squared of 0.9222 as listed in Table 4. Its position has an optimum position from RMSE position, Standard Deviation, and Coefficient Correlation as depicted in Figure 9, but in the prediction of infiltration rate it has RMSE 0.4927443 bigger than RMSE of model 6. This seems to be caused by two dots which are located far away from the line of accuracy as portrayed in Figure 10a. The most precise

model based on RMSE is model 6, where the dots scatter relatively close to the line of accuracy as depicted in Figure 10b. Nevertheless, this model has a weaker correlation between the dependent variable and independent variables which has the Multiple R Squared of the model is smaller than Model 1.

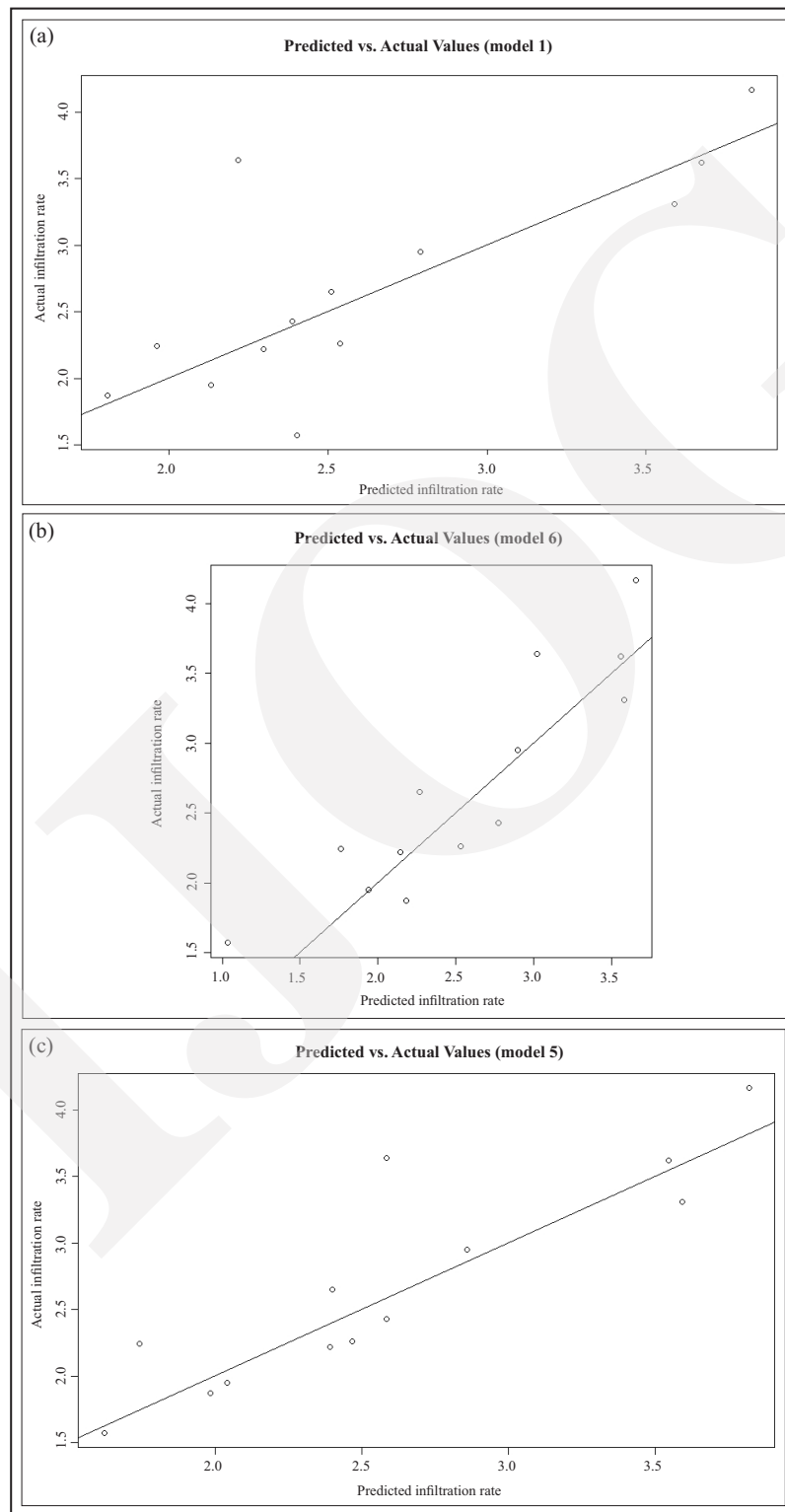$$y = 4.56992 - 0.03010x_1 - 0.083162x_2 \quad ....(6)$$

Figure 10. Plots of actual infiltration rate *versus* predicted infiltration rate (a) model 1, (b) model 6, and (c) model (5).

The comparison of observed and predicted infiltration rates based on the Model 6 has the RMSE value of 0.360245 and the MAE of 0.3022879. Based on the MAE values the most precise model is Model 5 which has an MAE of 0.2607738.

$$y = 0.621606 - 0.014539x_1 + 0.038490x_4 \quad \ldots\ldots\ldots(7)$$

On the other hand, the goodness of the model is mediocre compared to others as known from the MAE of 0.2607738 and its RMSE is 0.3683726. Its accuracy is illustrated in Figure 10c.

The contribution of each independent variable to the infiltration rate as depicted in Figure11.

can be described that the IWC, silt, and clay have negative correlations to the infiltration rate. While, sand has a positive correlation to the infiltration, and the correlation is reasonable. The presence of IWC will reduce infiltration having the initial moisture that will occupy void or pore spaces in the soil, and the presence of silt and clay material as a matrix between grain will reduce interconnected pores in the soil. Meanwhile, the greater presence of sand as grain and pebbles as fragment will increase the intergranular space ore pore space through which infiltration goes deeper in the ground.
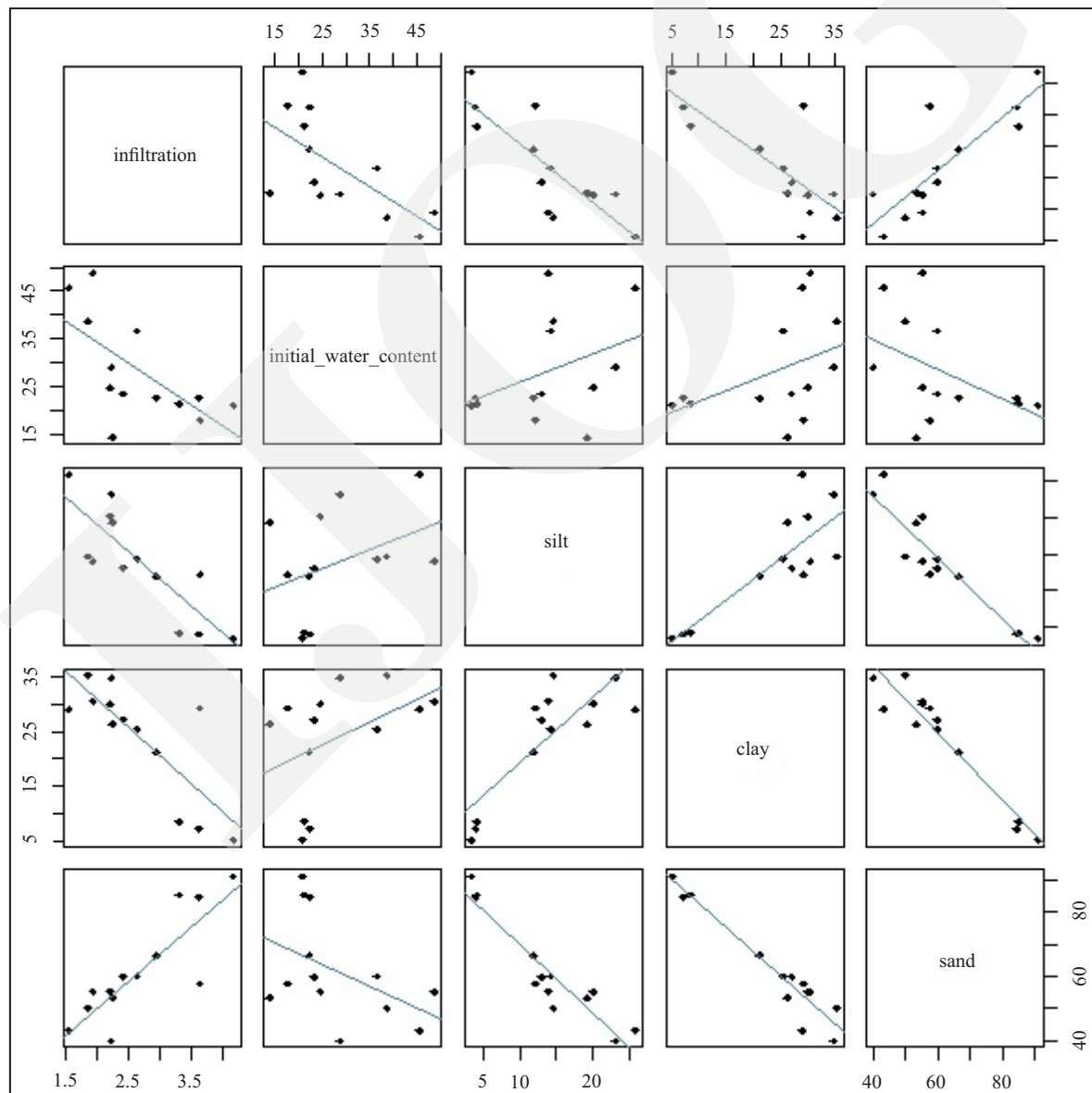

Figure 11. Pair diagram of soil parameters.

Conclusions

The correlation each of IWS, silt, and clay to the infiltration rate is negative where the greater of IWS, silt, and clay will reduce the infiltration rate of soil. Meanwhile, sand has a positif correlation to the infiltration rate. The bigger the amount of sand in soil, the bigger the infiltration rate in the soil. Eleven models regression have been developed using machine learning, and the fittest model of multiple regression based on Multiple R-Squared is Model 1 which takes all available parameters (IWC, silt, clay, and sand) as independent variables. Based on RSME, Model 6 has the greatest accuracy on this model parameters of sand, and clays are excluded. Meanwhile, based on MAE, Model 5 has the greatest accuracy and precision on this model, and the clay and silt are excluded. The regression Model 1 can be used to predict the infiltration rate on the studied area. For all parameters, the infiltration can also be obtained using Model 5 when available parameters are limited (IWC and sand percentage).

Acknowledgments

References

Alencoão, A.M.P. and Pacheco, F.A.L., 2006. Infiltration in the Corgo River basin (northern Portugal): coupling water balances with rainfall-runoff regressions on a monthly basis . *Hydrological Sciences Journal*, 51 (6), p.989-1005. DOI: 10.1623/hysj.51.6.989.

Angulo-Jaramillo, R., Bagarello, V., Iovino, M., and Lassabatere, L., 2016. *Infiltration Measurements for Soil Hydraulic Characterization*. Springer International Publishing. DOI: 10.1007/978-3-319-31788-5.

BAPPEDA Balikpapan, 2002. Kajian Geologi Untuk Evaluasi Penataan Wilayah dan Pengembangan Kota Balikpapan.

Bergeson, C.B., Martin, K.L., Doll, B., and Cutts, B.B., 2022. Soil infiltration rates are underestimated by models in an urban watershed in central North Carolina, USA. *Journal of Environmental Management*, 313, 115004. DOI: 10.1016/j.jenvman.2022.115004.

Bhave, S. and Sreeja, P., 2013. *ISH* Journal of Hydraulic Engineering Influence of initial soil condition on infiltration characteristics determined using a disk infiltrometer Influence of initial soil condition on infiltration characteristics determined using a disk infiltrometer. DOI: 10.1080/09715010.2013.808445.

Carslaw, D.C., 2019. The openair manual — open-source tools for analysing air pollution data. Manual for version 2.6-6, University of York.

Dahan, O., Shani, Y., Enzel, Y., Yechieli, Y., and Yakirevich, A., 2007. Direct measurements of floodwater infiltration into shallow alluvial aquifers. *Journal of Hydrology*, 344 (3-4), p.157-170. DOI: 10.1016/J.JHYDROL.2007.06.033.

Formansya, S., Gani, R.M., Firmansyah, Y., and Hermato, W., 2020. Sumberdaya Seam Batubara Formasi Pulau Balang di P.T. Anugerah Bara Kaltim, Kecamatan Loa Janan, Kabupaten Kutai Kartanegara, Kalimantan Timur. *Padjadjaran Geoscience Journal*, 4 (6). http://journal.unpad.ac.id/geoscience/article/view/32191/15018.

Fueki, N., Lipiec, J., Kuś, J., Kotowska, U., and Nosalewicz, A., 2012. *Soil Science and Plant Nutrition Difference in infiltration and macropore between organic and conventional soil management*. DOI: 10.1080/00380768.2011.644759.

Hidayat, S. and Umar. I., 1994. *Geological Map of The Balikpapan Quadrangle, Kalimantan, Scale 1 : 250.000.* https://geologi.esdm.go.id/geomap/pages/preview/peta-geologi-lembar-balikpapan-kalimantan.

Juwita, R. and Santoso, I.B., 2019. Assessment of Soil Infiltration Capability in Balikpapan City. *IPTEK Journal of Proceedings Series*,

0 (5), p.291-297. DOI: 10.12962/ J23546026. Y2019I5.6341.

Khosravi, K., Ngo, P.T.T., Barzegar, R., Quilty, J., Alami, M.T., and Bui, D.T., 2022. Comparing the Soil Conservation Service model with new machine learning algorithms for predicting cumulative infiltration in semi-arid regions. *Pedosphere*, 32, p.2-27.

Kiptiah, M., Azmanajaya, E., and Giarto, R.B., 2020. Analisis Laju Infiltrasi dengan Variasi Permukaan Tanah di Kota Balikpapan. *Jurnal Sipil Sains*, 10 (2), p.83-92. DOI: 10.33387/ SIPILSAINS.V10I2.2261.

Ma, J., Zeng, R., Yao, Y., Meng, X., Zhang, Z., Wang, H., and Zhao, S., 2022. Characterization and quantitative evaluation of preferential infiltration in loess, based on a soil column field test. *CATENA*, 213, 106164. DOI: 10.1016/J. CATENA.2022.106164.

McIntyre, D.S. and Sleeman, J.R., 1982. Macropores and hydraulic conductivity in a swelling soil. *Soil Research*, 20 (3), p.251-254. DOI:10.1071/SR9820251.

Michael, A.M., 2009. *Irrigation : theory and practice*. 768pp.

Muntohar, A.S., Ikhsan, J., Liao, H. J., Jotisankasa, A., and Jetten, V.G., 2022. Rainfall Infiltration-induced Slope Instability of the Unsaturated Volcanic Residual Soils During Wet Seasons in Indonesia. *Indonesian Journal on Geoscience*, 9 (1), p.71-85. DOI: 10.17014/ijog.9.1.71-85

Ruggenthaler, R., Meißl, G., Geitner, C., Leitinger, G., Endstrasser, N., and Schöberl, F., 2016. Investigating the impact of initial soil moisture conditions on total infiltration by using an adapted double-ring infiltrometer. *Journal*, 61 (7), p.1263-1279. DOI: 10.1080/ 02626667.2015.1031758.

Setiawan, O., Sartohadi, J., Pramono Hadi, M., and Mardiatno, D.. 2019. *Physical Geography Infiltration characterization using principal component analysis and K-means cluster analysis on quaternary volcanic landscape at the southern flank of Rinjani Volcano, Lombok Island, Indonesia*. DOI: 10.1080/02723646.2019.1620526.

Sihag, P., Singh, V.P., Angelaki, A., Kumar, V., Sepahvand, A., and Golia, E., 2019. Model-ling of infiltration using artificial intelligence techniques in semi-arid Iran. *Hydrological Sciences Journal*, 64 (13), p.1647-1658. DOI: 10.1080/02626667.2019.1659965.

Sugianti, K., Yunarto, Sadisun, I.A., and Kartiko, R.D., 2022. Analysis of Maximum-Rainfall-InfiltrationInduced Slope Stability Using the Transient Rainfall Infiltration and Grid-based Regional Slope-stability Model in Cililin, West Java, Indonesia. *Indonesian Journal on Geoscience, 9* (2), p.263-278. DOI: 10.17014/ ijog.9.2.263-278

Sulistyo, T., 2003. *Studi On Slope Stability In Vulnerable landslide Area For Evaluation Of General City Spatial Arrangement Plan In South Balikpapan* [UPN "Veteran" Yogyakarta]. http://opac.upnyk.ac.id/lib-sysintegrasi/opac/index.php/home/detail_ koleksi?kd_buku=00000000000000020017& id=1&title=Studi+On+Slope+Stability+In+V ulnerable+Landslide+Area+For+Evaluation+ Of+General+City+Spatial+Arrangement+Pla-n+In+South+Balik+Papan&kd_jns_buku=SK.

Sulistyo, T., 2018. *Identification Aquifer Parameters Through Single Well Pumping Test Series at PT. Kaltim Kariangau Terminal, Balikpapan, East Kalimantan*. 3 (2), p.293-300.

Sulistyo, T. and Abrar, A., 2017. Characterization of Thin Alluvial Bed Aquifers in Manggar River Balikpapan East Kalimantan Indonesia. *JTT (Jurnal Teknologi Terpadu)*, 5 (1), 54pp. DOI: 10.32487/jtt.v5i1.212.

Sy, N.L., 2006. Modelling the infiltration process with a multi-layer perceptron artificial neural network. *Hydrological Sciences-Journal-Des Sciences Hydrologiques*, 1, 51pp. DOI: 10.1623/hysj.51.1.3

Thomas, A.D., Austin, A., William, A., Eric, O.D., Alex, A.A., Maxwell, B., Isaac, L., Gilbert, A. A., and Duke, Q.N.D., 2022. Performance evaluation of infiltration models under different tillage operations in a tropical climate. *Scientific African*, 17, e01318. DOI: 10.1016/ J.SCIAF.2022.E01318.